Selective Light Emission in Nonbonding Electron Transitions in Poly(vinyl pyrrolidone) Molecules on Spin-Coating in Thin Layers

A. Mishra[†] **and S. Ram***

Materials Science Centre, Indian Institute of Technology, Kharagpur 721 302, India

Received: July 17, 2009; Revised Manuscript Received: November 4, 2009

It is shown that polymer molecules of poly(vinyl pyrrolidone) (PVP) rearranged in thin layers present surface-enhanced light emission in selective bands over a wide 260−860 nm range of spectrum. Four bands occur in spin-coated films by a dilute solution in water at 288, 395, 560, and 760 nm upon irradiating with an ultraviolet 200−250 nm light. The second and third bands are strong by contributing 82% intensity of the spectrum. Randomly dispersed PVP molecules in solution exhibit a single band (broad) at 425 nm {$\pi_0 \leftarrow n_1\pi_2^*$ transition in the nonbonding electrons n_1 in the C═O ($2s^2p^4$) group of pyrrolidone ring} and a harmonic band 650−860 nm (weak) of roughly twice its wavelength. In films, this band is split up into two well-separated $\pi_0 \leftarrow n_1\pi_2^*$ (395 nm) and $\pi_0 \leftarrow n_2\pi_1^*$ (560 nm) bands. Localized nonbonding electrons n_2 of the C−N ($2s^2p^3$) moiety of pyrrolidone ring excite and emit part of the energy in the $\pi_0 \leftarrow n_2\pi_1^*$ transition with as much intensity as in the $\pi_0 \leftarrow n_1\pi_2^*$ band. Localization of n_1 and n_2 electrons on molecular layers of films favors the resonance >N−C═O structure with three C═O stretching bands 1615, 1635, and 1665 cm^{-1} against a single band 1638 cm^{-1} in randomly dispersed molecules (solution). The C−N stretching frequency is decreased by 30 cm^{-1}. Results are useful for molecular designing of optical films for down-energy conversion, optical switching, and biological sensors.

1. Introduction

Radiative processes in conjugated polymer molecules such as poly(*p*-phenylene vinylene)s, poly(*p*-phenylene)s, poly(2,5-pyridine)s, polyfluorenes, or polythiophenes have been explored as active media in light-emitting devices.[1−8] Among such polymers, poly(2,5-pyridine)s and derivatives are known for highly efficient photoluminescence (PL) in the blue region.[2,4] Over the past few years, the search for PL of tunable visible colors has received considerable interest due to applications in optoelectronics,[9,10] photovoltaic cells,[11] biocatalysts,[12] biosensors,[10,13] and light-harvesting films.[14,15] Ram and Mondal have observed PL in planar molecules of poly(vinyl alcohol) (PVA) in dilute medium such as water.[16] Planar PVA molecule (isolated) has localized distribution of nonbonding (n) ö$^{2-}$ ($2s^2p^2$) electrons, which emit a visible light (n ← π^* transition). Occurrence of radiative emission in aqueous medium is useful for designing optical films from dispersed molecules in solution. Conjugated polymers combine light-emission properties with polymer processability, band-gap tunability, and mechanical flexibility as per the molecular structure.[17,18] A coplanar structure of the polymer backbone through covalent bond modifications or H-bonding is believed to promote radiative emission.[10,19] Doping of electrons or holes sensitively tailors optical properties with modified thermal (or electrical) conductivity, biological reactivity, and other useful properties in a single system.

Poly(vinyl pyrrolidone) (PVP) is a medical compound for targeted drug delivery, therapeutic agents, tablet disintegrating agents, lubricator and antitoxic assistant for drugs, bladder cancer detection and diagnosis, artificial cartilages in cartilages replacement, etc.[20−23] PVP molecules of molecular weight M_w ~ 40 000 or lower can be dispersed in single molecules in water of dilute solution in such applications. As electron donors, they lower the valence states of noble metal ions and cadge them in nanoclusters of distinctive color of an optical nanofluid for biological sensors[24−27] and other applications.

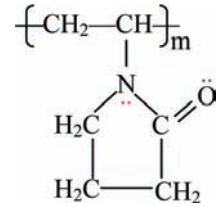

Figure 1. Molecular structure of a monomer which recombines one after other in number *m* in a PVP polymer layer under specific conditions. C═O and C−N moieties carry n_1 ($2p^2$) and n_2 ($2s^2$) nonbonding electrons, respectively.

We observed that PVP molecules dispersed in hot water shine violet-blue and red lights when irradiating in the absorption band 200−350 nm, which varies in position and/or intensity nonlinearly with the concentration (0.1−10 g/dL).[26,27] Excited sample appears blue to the naked eye. Fujihara and Kitta[28] observed a broad emission 400−600 nm in PVP/silica films of dip-coating on a silica glass and annealed at 250 °C for 10 min in N_2 gas. In this article, we report PL emission with the role of layered molecules in radiative processes in thin PVP films. As described with proposed energy level diagrams, localized n electrons in C═O and C−N moieties of pyrrolidone ring emit in multiple bands in the visible−near-infrared region useful for several applications.

2. Experimental Details

The PVP films (molecular structure in Figure 1) were prepared from a spectroscopic grade compound (M_w ~ 40 000

* To whom correspondence should be addressed. Phone: (091) 3222 283980 (O); 283981 (R). Fax: (091) 3222-255303. E-mail: sram@matsc.iitkgp.ernet.in.
† Present address: Department of Physical Chemistry II, Ruhr-University Bochum, 44780 Bochum, Germany.

10.1021/jp906765x
Published on Web 12/02/2009

g/mol and polymerization number $m = 360$) from Aldrich chemicals. Polymer layers as long as 100−200 nm can be formed out of it assuming a size of monomer of 0.3−0.5 nm. Such molecules were obtained by mechanochemical stirring a dilute solution as follows. A 100 mL solution was obtained in 10 g of PVP in distilled water by magnetic stirring in a beaker for 2 h at room temperature followed by 2 h at 50−60 °C. In hot conditions, molecular stretching extends surfaces on single PVP molecules,[16] with as high transmittance of sample as ∼90% in the visible region. It was spin-coated as a thin film (a circular shape of 2 cm diameter and 2 μm thickness) over a quartz plate and ultimately dried in a vacuum. A spin-coater of Apex SCU 2005 has been used. During the process, the film was spinning with an angular velocity 20 cycles s^{-1} (i.e., as high as 1.3 m s^{-1} linear velocity at the film circumference). Microscopic images recorded with a scanning electron microscope (Oxford Model Leo 1550) ensure a liquidlike structure of films with highly smooth surfaces. The amorphous nature of films was studied in terms of X-ray diffraction (XRD) using a Phillips PW 1710 X-ray diffractometer with a 0.15418 nm Cu Kα radiation.

The PL and excitation spectra have been recorded of films and parent solution with a computer-controlled Perkin-Elmer (Model-LS 55) luminescence spectrometer in conjugation with a red sensitive PMT detector (RS928) and a high-energy pulsed xenon discharge lamp as an excitation source (average power 7.3 W at 50 Hz). A quartz cell of 10 mm width hosted the liquid sample. The spectra have been scanned at a rate 500 nm/min with ∼10 nm widths for the entrance or the emission slit. Infrared spectra have been studied for powder, solution, and films from PVP molecules with a Thermo Nicolet Corporation Fourier Transform Infrared Spectrometer (Model NEXUS-870). The spectrum from solution has been recorded in an attenuated total reflectance (ATR) mode using a ZnSe crystal as a sample holder. Putting a few drops (1−2 μL) of the solution over the crystal results in a film of the sample which adheres to the ATR crystal. Raman spectra were measured on a Renishaw inVia Raman spectrophotometer with a 514.5 nm Ar^+ ion laser.

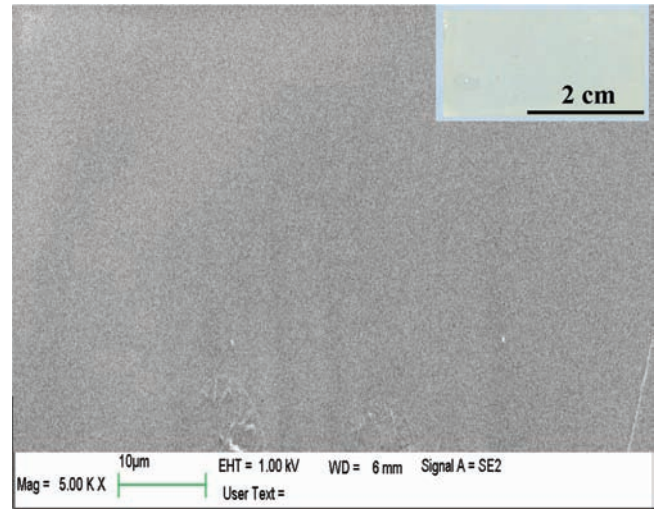

Figure 2. SEM microstructure of a spin-coated PVP film on a quartz plate of photograph given in the top in which the sample is laying on a paper (bluish color).

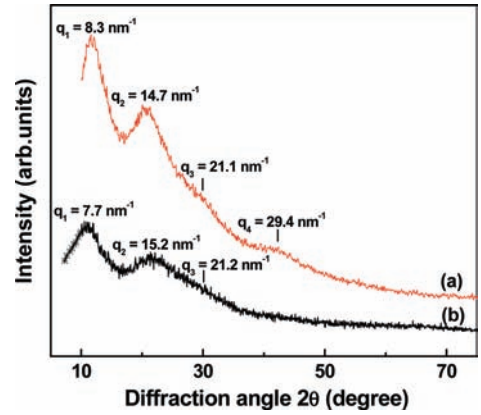

Figure 3. X-ray diffraction patterns in (a) the films and (b) the starting PVP powder.

3. Results and Discussion

3.1. Molecular Structure in PVP Films. In the course of spin-coating on a quartz plate, dispersed PVP molecules in hot water (on prolonged mechanical stirring) deposit in molecular layers along the plate in the form of a thin film. In spinning at 20 cycles s^{-1}, or as high a linear velocity of the film circumference as 1.3 ms^{-1}, used in this experiment, the polymer molecules in wet film are stretched in extended surfaces in individual molecules and those are ultimately arranged along the film surface. In an ideal case, layers as thin as a single molecule (on the order of 0.2 nm) constitute such films. A typical micrograph in Figure 2 presents a fairly smooth surface at the micrometer scale throughout the film. It implies that molecular PVP films lay down uniformly one over another in a systematic manner. A colorless transparent film can be seen from a photograph in the top in Figure 2 in which it is laying on a bluish paper showing the contrast.

The XRD pattern in Figure 3a consists of four halos of wave vectors $q_1 = 8.3$, $q_2 = 14.7$, $q_3 = 21.1$, and $q_4 = 29.4$ nm^{-1}, characterizing a semicrystalline structure of the PVP films. A bit different values $q_1 = 7.7$, $q_2 = 15.2$, and $q_3 = 21.2$ nm^{-1} in the starting powder (Figure 3b) confer that the constituent atoms C, O, and N are rearranged in films in four primary pair distributions. H atoms are too small to affect the distribution at this scale. PVP molecules in a layer are assuming reasonably larger q_1 value, i.e., ∼6.5% smaller value of the average interatomic distance. A similar XRD pattern with $q_1 = 8.2$ and $q_2 = 14.9$ nm^{-1} is reported in Au-nanoparticles (0.1−0.5 wt %) reinforced PVP molecules of a composite.[29]

A coplanar pyrrolidone ring with the side groups in a monomer (Figure 1) can design a polymer layer in several ways as per the m value. Small PVP molecules, 100−200 nm long chains ($m = 360$) in this experiment, are taken as planar in practical purpose of films. In a stable conformation, the side groups can adopt s- and i-dyads in generating an eclipsed arrangement of backbone N−CH_2 or N−(C═O) and the C−H bonds. Three kinds of most preferable conformers (a) s-PVP-1, (b) s-PVP-2, and (c) s-PVP-3 shown in Figure 4 share strong intermolecular intercalations which support them not only on stereosequence but also on the side group orientations in a polymer chain. From a symmetry point of view, other conformers are not so stable in small chains without involving such extensive H-bonding. As marked by the area ABCD in Figure 4 in a group of $m = 4$ monomers, a molecular s-PVP-1 layer describes a maximal surface charge density on $2p^2$(O) and $2s^2$(N) n electrons. As can be analyzed by the molecular geometry,[26] it is as large as ∼1.5 times the value in s-PVP-2 or 3 (equal surfaces). Nearly equal surfaces in the C═O and C−N moieties support resonance electronic structure in the n electrons (Figure 5). As an activated electron donor, the C═O donates an n electron (n_1) to the neighboring N atom (electron acceptor) in

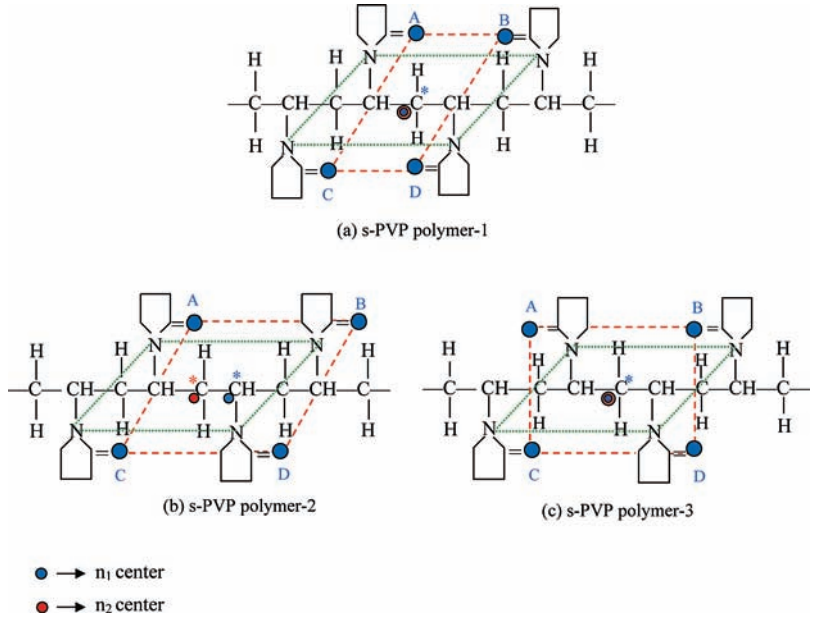

Figure 4. Three kinds of the most preferable conformers (a) s-PVP-1, (b) s-PVP-2, and (c) s-PVP-3 of a PVP molecule of a thin layer.

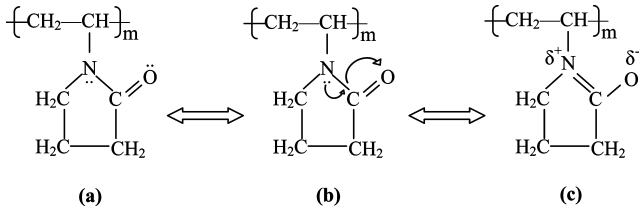

Figure 5. Resonance structure with delocalized n_1 and n_2 electrons on planar pyrrolidone ring in PVP monomer. (a) n_1 electrons on the C−N moiety displace toward (b) the C═O moiety such that it causes (c) charge centers.

the >N−C═O moiety in a kind of an intramolecular charge transfer. High polarity developed in monomer units in this resonance structure facilitates interbridging them in a polymer layer.

In both s-PVP-2 and s-PVP-3, the C−N moiety is sharing nearly 10% smaller surface area, i.e., larger surface charge density than the C═O moiety. The C−N n electrons (n_2) dominate the resonance >N−C═O structure (Figure 5c). The s-PVP-2 differs from s-PVP-3 in the molecular (*) as well as the charge center (●) in Figure 4. Such parameters are common in s-PVP-1 and s-PVP-3 conformers. As will be discussed later, these conformers have distinct bond-stretching frequencies. In the models in Figure 6a−d in thin films, the conformers arrange one over another perpendicular to the film surface (z axis). In this configuration, n_1 and n_2 electrons are laying in parallel arrays. Such molecules thus embed these electrons in individual molecular layers (Figure 6b) of a self-localized electronic structure on the parent >N−C═O moieties. Monomers lying one over another in a group of two are shown in Figure 6c along with a general configuration in Figure 6d, showing a polymer bed with n_1 and n_2 electrons (Figure 6e). As will be discussed further, a specific electronic structure in a specific conformer describes a characteristic electronic spectrum of radiative emission.

A stable conformer s-PVP of planar surfaces selectively adsorbs metal ions, atoms, or molecules on the C═O sites useful in surface-enhanced biological reactions. As a molecular template, it drives directional growth in nanowires of gold, silver, and similar metals from a salt in water.[24,30,31] s-PVP

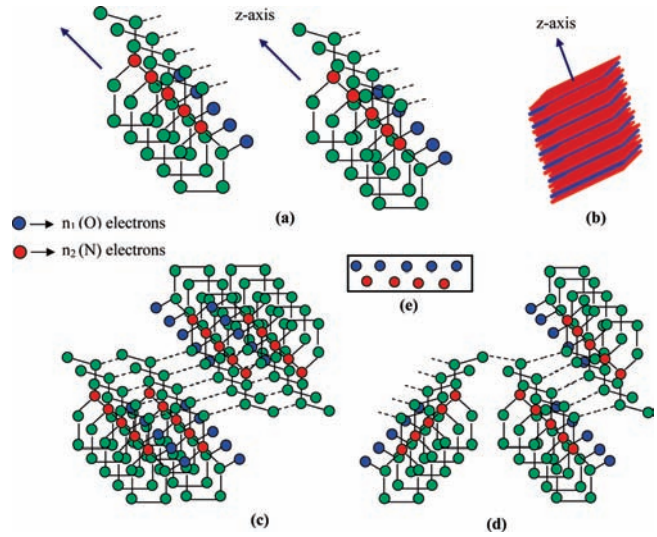

Figure 6. Model molecular layers on aligned molecules in thin PVP films: (a) single monomers lying one over another along the z axis (perpendicular to the film), (b) layers consisting of n_1 and n_2 electrons, (c) dimers lying one over another, (d) a general configuration with monomer or polymer units, and (e) a polymer bed with n_1 and n_2 electrons.

selectively interacts with a growing lattice in the {111} facets, with unusual pentagonal cross sections of nanowires in a conformer-dependent interaction in a topotactic reaction. It opens a platform 1;to develop (i) mechanisms of how PVP molecules react with kinds of reaction species and (ii) underlying processes in biomaterials, medicines, biosensors, optical systems, or other devices.

3.2. Radiative Emission in PVP Films. The spin-coated PVP films emit four well-separated bands of average peak values (λ_{em}) 288, 395, 560, and 760 nm in Figure 7a when irradiating at wavelength λ_{ex}-250 nm of excitation maximum. Normalized peak intensities (I_p) vary in these bands in the order 21:100: 54:13, respectively. In analyzing the successive emission processes in the four bands, we studied excitation spectra by exciting at selective λ_{em} values. The excitation spectra scanned for the emission bands 395, 560, and 760 nm are compared in Figure 7b−d. Exciting at the 288 nm emission exhibits similar

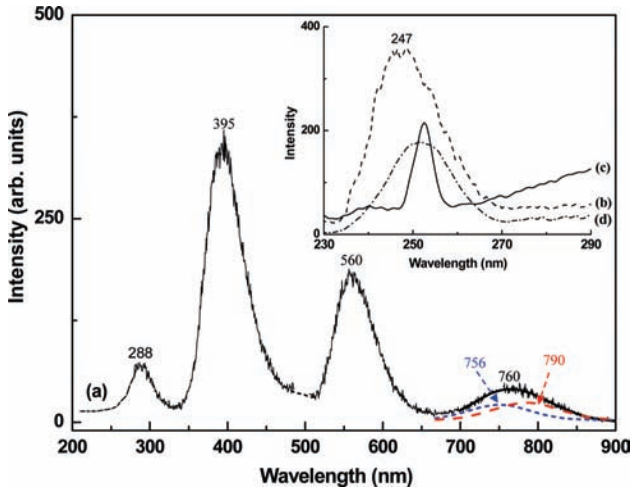

Figure 7. (a) Light emission ($\lambda_{ex} = 250$ nm) and the excitation spectra monitored at (b) 395, (c) 560, and (d) 750 nm of emission bands in spin-coated PVP films. A dashed line is incorporated in spectrum (a) after removing the first harmonic of the λ_{ex} value.

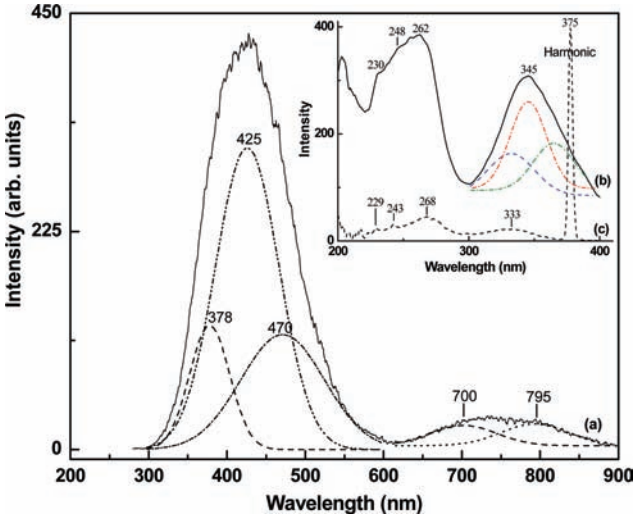

Figure 8. (a) Light emission ($\lambda_{ex} = 250$ nm) and the excitation spectra monitored at (b) 425 nm and (c) 750 nm of emission bands in PVP molecules in water.

a spectrum as shown for the 560 nm emission band. The prominent excitation process of electrons that spans a broad band 230−270 nm is emitting light strongly in the 395 nm band followed by part of the energy in the 760 nm band (weak) in a common origin of photons of PVP molecules. Having roughly twice the λ value of the first band the long wavelength band can be treated as its harmonic (first order).

A single band group (Figure 8a) occurs of a different spectrum over 300−600 nm {∼125 nm of the full-width at half-maximum (fwhm)} in PVP molecules in the solution before spin-coating as films. A harmonic band group 600−900 nm (fwhm ∼ 160 nm) persists with an order of lowered I_p value. As expected, excitation spectra differ in the two emission bands mainly in the intensities. An excitation spectrum (Figure 8b) in primary emission band ($\lambda_{em} = 425$ nm) exhibits an order of larger intensity of those (Figure 8c) in the harmonic band. Two groups 225−300 and 300−400 nm arise of nearly equal excitation intensities. Four bands 230, 248, 262, and 345 nm of the spectrum in Figure 8b are modified to 229, 243, 268, and 333 nm on modifying emission profiles in Figure 8c in the harmonic bands. Manzoor et al. observed a similar excitation spectrum (for the emission band at 430 nm) of four bands 235, 260, 340, and 374 nm in a rather dilute 1 g/dL PVP sample in water.[32] Conformers govern selective excitation and emission processes as per the experimental conditions.

As shown in Figure 8a, a deconvolution describes the violet-blue emission 300−600 nm in terms of three distinct bands of peak positions 378, 425, and 470 nm, with an average 425 nm value. Values for fwhm and peak intensity in these bands are given in Table 1. Phenomenologically, the longest wavelength band 470 nm ascribes to s-PVP-1 conformer, while those of smaller values 425 and 378 nm arise in s-PVP-2 and s-PVP-3, respectively, which do not involve such strong interchain bridging and internal interactions (Figure 4). This is according to average charge densities in C═O and C−N n-electrons on the surface ABCD. The average C═O charge center (also the mass center) in s-PVP-2 stays close to one of the N sites in groups of four nearest neighboring ones so that it receives the electron transfer. Effectively longer wavelength arises in easing $n_2 \leftarrow n_2\pi^*$ electronic transition above the s-PVP-3 value wherein the average C═O charge center stays a bit away from the nearest N site. An electric dipole on separated average charge centers on C═O and C−N moieties renders highly emissive $n_2 \leftarrow n_2\pi^*$ transition in this specific conformer. As illustrated in Figure 9, three kinds of excited levels $n_1\pi_1^*$, $n_1\pi_2^*$, and $n_1\pi_3^*$ primarily in C═O n_1 electrons emit the light in steps via excited states on π electrons in the selective PVP conformers.

The energy level diagram in Figure 10 describes how the s-PVP-3 conformer conducts λ doubling of the primary 378 emission band in two distinct bands 700 and 795 nm. A photon of energy $2\,h\nu_1$ from 378 nm light emission recombines a phonon υ_1 in an s-PVP-3 molecule, populating a υ_1-supported state $n_1\pi_1^*$ of energy $2h\nu_1 + \upsilon_1$. The energy relieves in parts BC and CD in two emission bands of energies $h\nu_1 + \upsilon_1$ and $h\nu_1$ as follows:

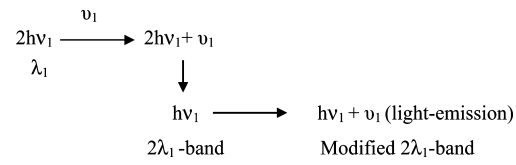

A modified harmonic band 700 nm (from the ideal value 756 nm) of energy $h\nu_1 + \upsilon_1$ appears in a preferred $\pi_o \leftarrow n_1\pi_1^*$ transition on the electron−phonon mixing, assuming a value $\upsilon_1 = 1058$ cm^{-1} observed in the C−N stretching vibration.

TABLE 1: Electronic Transitions in $\pi \leftarrow n_1\pi_{1-3}^*$ Band Group in *s*-PVP Molecules in Water[a]

band	λ_{max} (nm)	intensity*	energy (cm^{-1})	fwhm (nm)	assignment
band 1	378	40.8	26 455	51.3	$\pi \leftarrow n_1\pi_1^*$ s-PVP-3
band 2	425	100	23 529	81.2	$\pi \leftarrow n_1\pi_2^*$ s-PVP-2
band 3	470	37.7	21 276	106.9	$\pi \leftarrow n_1\pi_3^*$ s-PVP-1
band 4	700	7.7	14 286	84.4	modified harmonic (band 1)
band 5	795	7.3	12 578	85.7	modified harmonic (band 2)

[a] Normalized values at a scale of 100 units.

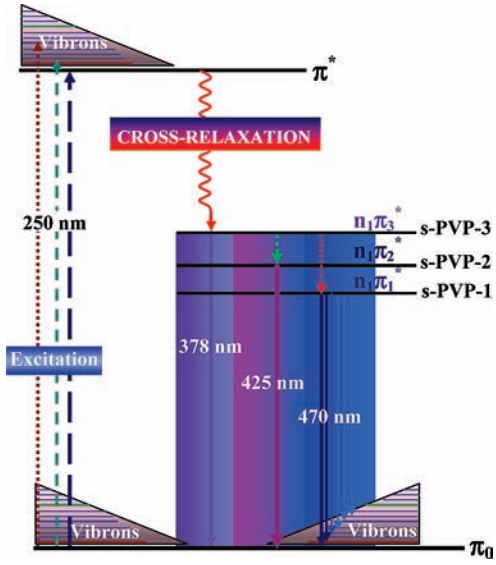

Figure 9. Model energy level diagram illustrating the light emission (through an excitation π^* state) in $n_1\pi_3^*$, $n_1\pi_2^*$, and $n_1\pi_1^*$ electronic states in three conformers s-PVP-3, s-PVP-2, and s-PVP-1 in water according to the spectrum observed in Figure 8.

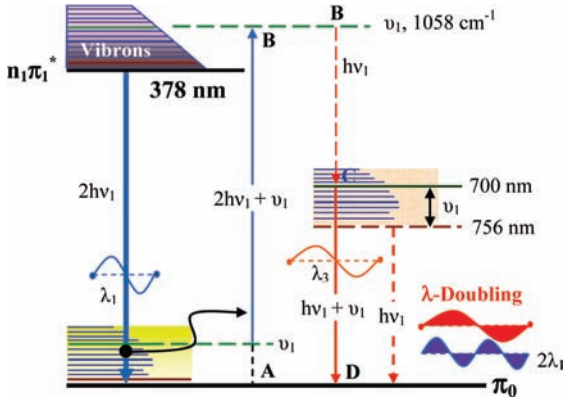

Figure 10. Model energy level diagram describing degeneration of two emission bands 700 nm (λ_3) and 756 nm ($2\lambda_1$) from a single photon of 378 nm light emission (λ_1) in s-PVP-3 molecules in water. A phonon 1058 cm^{-1} of the C−C chain deformation mediates the process.

Similarly, the υ_1 band on mixing with the $\pi_o \leftarrow n_1\pi_2^*$ transition at 425 nm (s-PVP-2 conformer) describes the other harmonic band 795 nm. In both the examples, the final light emission dominates over the parent harmonic generation ($\upsilon_1 = 0$). A thin conformer layer of small PVP molecules serves as an λ_{ex} resonator, promoting the $n_1\pi_1^*$ and $n_1\pi_2^*$ population inversions via a resonance excitation $\pi_0 \rightarrow \pi^*$ (Figure 9). Nevertheless, more vibronic bands, which share an extended fwhm value 107 nm, inhibit the λ-doubling process on the part of energy loss in the 470 nm emission in s-PVP-1 conformer. Vibronic levels in the ground electronic state mediate releasing energy of excited photons in vibronic transitions, i.e., an electron → phonon energy transfer.

Light emission in two well-separated bands of 395 and 560 nm in films in Figure 7 confers that they consist of planar s-PVP-2 and s-PVP-1 conformers. Low-energy phonons still persist in asymmetric band shape on the longer wavelength side. As demonstrated in Figure 11, two transitions $\pi_o \leftarrow n_1\pi_2^*$ and $\pi_o \leftarrow n_2\pi_1^*$ arise in the two conformers, respectively. A preponderance of n_2 electrons (N) in a resonance >N−C═O structure accounts for a lower energy in the s-PVP-1 conformer (Figure 4a). A poor ultraviolet emission around 288 nm ($\pi_o \leftarrow$

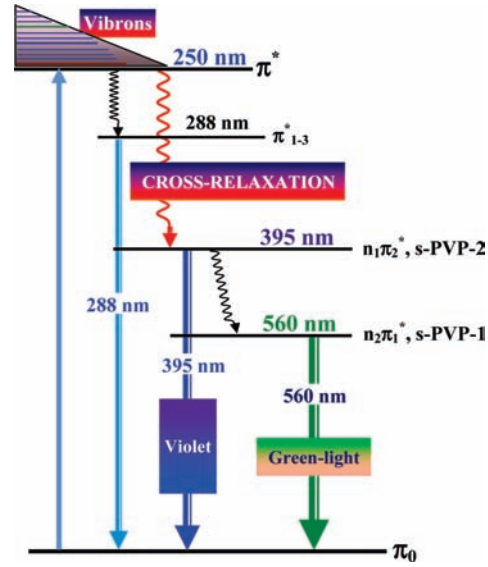

Figure 11. Model energy level diagram illustrating a four-step emission process with three intermediate electronic states π^*_{1-3}, $n_1\pi_2^*$, and $n_2\pi_1^*$ in thin films of PVP molecules according to the spectrum observed in Figure 7.

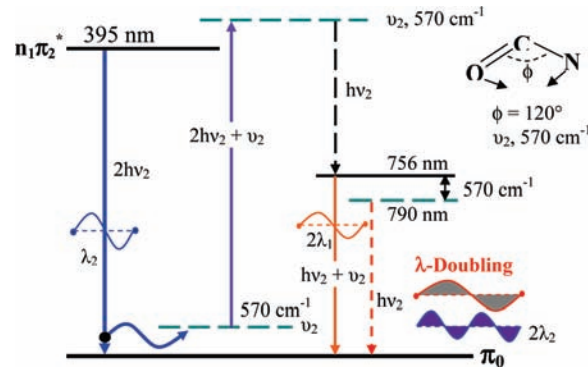

Figure 12. Model energy level diagram describing degeneration of two emission bands 756 nm ($2\lambda_1$) and 790 nm ($2\lambda_2$) from a single photon of 395 nm light emission (λ_2) in thin PVP films. A phonon 570 cm^{-1} of the >N−C═O angle bending mediates the process.

π_{1-3}^* transition) is characteristic of exciting π electron from the pyrrolidone ring. It is an induced transition on a resonator with the $\pi_o \leftarrow n_2\pi_1^*$ transition of 560 nm, i.e., a nearly multiple λ_{em} value $2 \times 288 = 576$ nm. n_2 electrons of enhanced surface density tailor π electrons to be coplanar to the monomer. As described in Figure 12, in a down-energy conversion in the $\pi_o \leftarrow n_1\pi_2^*$ transition, a phonon υ_2 leads an excited photon $2h\nu_2$ to split into two emission bands of energies $h\nu_2 + \upsilon_2$ and $h\nu_2$:

$$2h\nu_2 \xrightarrow{\upsilon_2} 2h\nu_2 + \upsilon_2 \rightarrow h\nu_2 + \upsilon_2 \text{ (light-emission)}.$$

($2\lambda_2$ band; Modified $2\lambda_2$-band)

The modified $2\lambda_2$ band 756 nm with $\upsilon_2 = 570$ cm^{-1}, >N−C═O angle bending in pyrrolidone ring, has enhanced intensity of the parent harmonic band 790 nm.

A comparison of emission in PVP molecules in selective forms (Table 2) envisages that a molecular layer tailors surface-enhanced emission in three primary 395 nm (violet), 560 nm (green), and 760 nm (red) colors. Red emission is useful for

TABLE 2: PL Emission in PVP Molecules of Confined Molecular Structure in Selective Forms[a]

sample	λ_{em} (nm) band 1	band 2	band 3	ref
10 g/dL PVP in water	378(40.8)	425(100)	470(37.7)	present work
spin-coated PVP films	288(20.9)	395(100)	560(53.8)	present work
1 g/dL PVP in water	390(82.4)	430(100)	475(70.6)	32
PVP/SiO_2 hybrid films		440(100)		28

[a] Normalized peak intensities are given in parentheses.

optical imaging and curing cancer tissues. Endogenous tissue chromophores stay safely from radiation absorption in this region. Such PVP molecules are promising fluorophores for fluorescence diagnosis in in vivo fluorescence imaging and optical detection of human cancer tissue: a subject of immense biological studies and biomedical applications.[33−35] A photosensitizer chlorin e6 with PVP molecules serves as a good exogenous fluorophore in imaging human cancer tissue.[35] In a human body, a tablet inside PVP molecules can be identified in the emission. Chen et al. observed that when adding to a red light-emitting diode PVP molecules promote 750 nm red emission in a proximity sensor.[36]

3.3. Phonons in Electron−Phonon Mixing in PVP Molecules. We studied phonon bands in characterizing electron−phonon mixing in selective conformers in thin PVP films. The C−N stretching, C═O stretching, and angle bending describe three primary bands in the >N−C═O moiety in a conformer. In Figure 13a, b, a doublet of Raman bands at 570 and 650 cm^{-1} in the >N−C═O angle bending vibration υ_2 describes that the >N−C═O unit is lying in two conformers s-PVP-1 and s-PVP-2, respectively. s-PVP-1 on effectively smaller separation between successive >N−C═O units in a polymer has a smaller υ_2 value. As inferred from the emission bands, this specific vibration offers peculiarly a strong electron−phonon coupling with a resolved vibronic band in stabilizing these polymer conformers. Randomly dispersed PVP molecules no longer show such a distinct band out of this vibration in solution (Figure 13c). A sharp intense band 1120 cm^{-1} (C−C chain stretching) occurs superposing over a broad band at 1058 cm^{-1} (stretching in the C−N bond connecting the chain). IR spectra (d, e) in Figure 13 reveal a group of three bands 755, 760, and 765 cm^{-1} in the C−C chain deformation in s-PVP-1, s-PVP-2, and s-PVP-3 conformers, respectively, in a sequence of the model surface charge density and emission bands. Conformer s-PVP-2, which is the most intense light emitter, exhibits the most intense IR band. As described above, these specific phonons offer electronic coupling that tailors selective light emission bands with resolved vibronic bonds of them in these three PVP conformers.

Markedly different IR bands in intensities (Figure 14) from the Raman bands (Figure 13a) confer that films have PVP molecules configured in symmetric shapes (planar). Symmetric (asymmetric) vibrations appear in strong (weak) Raman bands while weak (strong) IR bands and vice versa.[33,37] Most of them are of doublet or triplet structure on PVP molecules lying in two and/or three distinct conformers. A close-up of C═O stretching vibration (Figure 14b) reveals three bands 1615, 1635, and 1665 cm^{-1} (a single band mixed-up with H_2O bending vibration in the solution at 1638 cm^{-1}), which are assigned to s-PVP-3, s-PVP-2, and s-PVP-1 conformers, respectively, in an opposite trend to the in-plane bending or deformation vibrations. The corresponding C−N stretching values are 1245, 1280, and 1325 cm^{-1} (1275, 1295, and 1320 cm^{-1} in the solution in Figure 13f), respectively. A presumably >N−C═O resonance

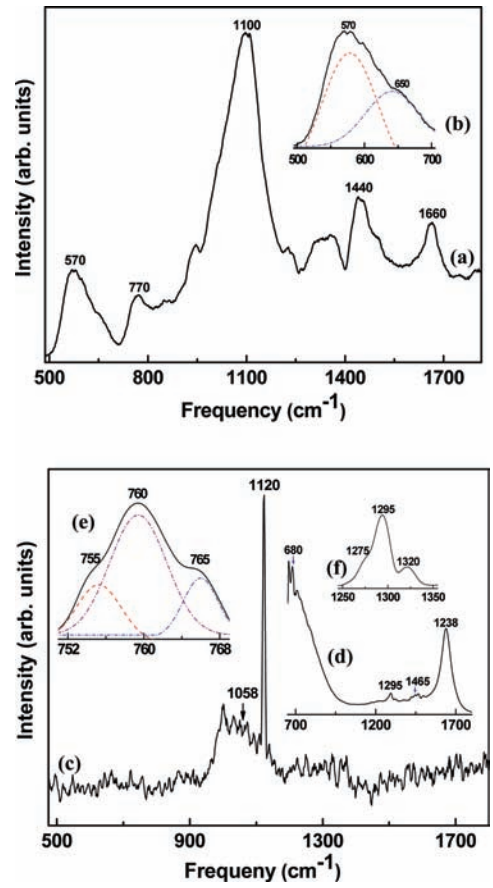

Figure 13. Raman (a−c) and IR spectra in PVP film (a, b) and aqueous solution (c−f) used to obtain the film. High-resolution spectra in the insets demonstrate a doublet (b) and a triplet (e) or (f) band structure in the preferred conformers.

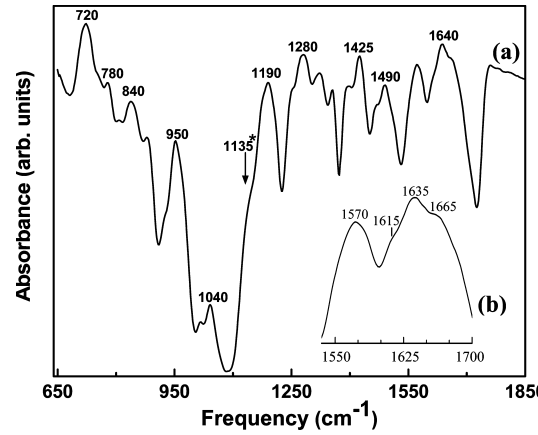

Figure 14. (a) IR spectrum of PVP films with (b) part of a close-up of the C═O stretching band in three PVP conformers. *C−C stretching in the pyrrolidone ring.

structure causes only weak Raman bands in C═O or C−N stretching. Moreover, a strong Raman band 1100 cm^{-1} in the C−C stretching has a counterpart IR band 1135 cm^{-1} of only weak intensity, a shoulder to a strong band 1190 cm^{-1} in the CH_2 twisting.

In the model conformers in Figure 6, the localized n_1 and n_2 electrons in molecular PVP layers certainly ease the stretching bands of the C═O and C−N bonds, and those account for the intensified emission bands in the $\pi_0 \leftarrow n_1\pi_{1,2}^*$ and $\pi_0 \leftarrow n_2\pi_2^*$ transitions (Figure 7). As described above in section 3.2, a wide patch of inseparable phonon bands in general extends up to

± 3000 cm^{-1} from the (0, 0) emission peak value, diverging the features of an asymmetric profile over the λ-longer side. Otherwise, a pure electronic transition is pretty sharp. Nevertheless, such high-energy phonons are not so commensurate for executing the λ-doubling process because of preferred relaxation to lower energy phonon levels. They simply mediate the excited photons of releasing part of the energy rapidly via the vibronic levels in the ground electronic state, i.e., usual electron → phonon energy transfer.

4. Conclusions

When spin-coating (a dilute sample 10 g/dL or lower in water) conjugated polymer PVP molecules rearrange in layers in selective conformers. Four halos of X-ray diffraction occur of wave vectors 8.3, 14.7, 21.1, and 29.4 nm^{-1} in four kinds of atomic distributions. The halo 29.4 nm^{-1} describes reflections from molecular layers of 0.214 nm thickness. Preferred conformers s-PVP-1, s-PVP-2, and s-PVP-3 in films tailor surface-enhanced emission in three bands 288, 395, and 560 nm on excitations of π electrons (pyrrolidone ring) and nonbonding electrons n_1 and n_2 in the C═O and C−N moieties. A resonance >N−C═O structure with localized n_1 and n_2 electrons in such conformers results in separate $\pi_0 \leftarrow n_1\pi_2^*$ (395 nm) and $\pi_0 \leftarrow n_2\pi_1^*$ (560 nm) bands of nearly equal intensities. Only one band occurs at 425 nm ($\pi_0 \leftarrow n_1\pi_{1-3}^*$) in randomly dispersed PVP molecules. Model electronic energy levels describe the transition processes in model conformers.

Thin layers of small PVP molecules serve as a wavelength λ_{ex} resonator so that they emit light in exciting n_1 and n_2 electrons out of a self-confined >N−C═O structure. This selective emission in n_1 and n_2 electrons is due to a combination of the resonance excitation in the π^* electronic band and charge transfer enhanced $\pi_0 \rightarrow \pi^*$ excitation spectrum. These specific conditions are achieved by (i) the 200−250 nm light for the excitation from a xenon source, (ii) an increase of the C═O stretching band on the order of 27 cm^{-1} in $n_2 \rightarrow n_1$ electron transfer, and (iii) electron−phonon coupling with selective phonons. Coplanar PVP conformers have the C−C stretching (chain) of a strong Raman band 1100 cm^{-1}. Three identified conformers s-PVP-1, s-PVP-2, and s-PVP-3 in the light emission have distinctive IR/Raman bands in the C═O, C−N, or other group vibrations. Molecular designing of such polymer molecules tailors functional optical properties for wave guides, optical films, optical switching, biosensors, or other possible applications.

Acknowledgment. This work has been support in part by the University Grant Commission, New Delhi, and the Department of Atomic Energy, Government of India.

References and Notes

(1) Tessler, N.; Harrison, N. T.; Friend, R. H. *Adv. Mater.* **1998**, *10*, 64.
(2) Cerullo, G.; Stagira, S.; Nisoli, M.; De Silvestri, S.; Lanzani, G.; Kranzelbinder, G.; Graupner, W.; Leising, G. *Phys. Rev. B* **1998**, *57*, 12806.
(3) Leclerc, M. *Adv. Mater.* **1999**, *11*, 1491.
(4) Nisoli, M.; Stagira, S.; Rossi, M.-Z.; De Silvestri, S.; Mataloni, P.; Zenz, C. *Phys. Rev. B* **1999**, *59*, 11328.
(5) Setayesh, S.; Marsitzky, D.; Mullen, K. *Macromolecules* **2000**, *33*, 2016.
(6) Herz, L. M.; Philips, R. T. *Phys. Rev. B* **2000**, *61*, 13691.
(7) Khan, A. L. T.; Sreearunothai, P.; Herz, L. M.; Banach, M. J.; Köhler, A. *Phys. Rev. B* **2004**, *69*, 085201.
(8) Schwartz, B. J. *Nat. Mater.* **2008**, *7*, 427.
(9) Ispasiu, R. G.; Balogh, L.; Varnavski, O. P.; Tomalia, D. A.; Goodson, T. *J. Am. Chem. Soc.* **2000**, *122*, 11005.
(10) Baskar, C.; Lai, H. Y.; Valiyaveettil, S. *Macromolecules* **2001**, *34*, 6255.
(11) Halls, J. J. M.; Walls, C. A.; Greenham, N. C.; Marseglia, E. A.; Friend, R. H.; Moratti, S. C.; Holmes, A. B. *Nature* **1995**, *376*, 498.
(12) Szczesna, M.; Galas, E.; Bielecki, S. *J. Mol. Catal. B* **2000**, *111*, 671.
(13) Heeger, P. S.; Heeger, A. *Proc. Natl. Acad. Sci. USA* **1999**, *96*, 12219.
(14) Schenning, A.; Peeters, E.; Meijer, E. W. *J. Am. Chem. Soc.* **2000**, *122*, 4489.
(15) Hecht, S.; Frechet, J. M. J. *Angew. Chem., Int. Ed.* **2001**, *40*, 74.
(16) Ram, S.; Mondal, T. K. *Chem. Phys.* **2004**, *303*, 121.
(17) Graupner, W.; Cerullo, G.; Lanzani, G.; Nisoli, M.; List, E. J. W.; Leising, G.; De Silvestri, S. *Phys. Rev. Lett.* **1998**, *81*, 3259.
(18) Park, J.; Park, S. Y.; Shim, S.-O.; Kang, H.; Lee, H. H. *Appl. Phys. Lett.* **2004**, *85*, 3283.
(19) Nakazawa, M.; Han, Y. K.; Fu, H.; Matsuoka, S.; Kwei, T. K.; Okamoto, Y. *Macromolecules* **2001**, *34*, 5975.
(20) Kamada, H.; Tsutsumi, Y.; Kamada, K. S.; Yamamoto, Y.; Yoshioka, Y.; Okamoto, T.; Nakagawa, S.; Nagata, S.; Mayumi, T. *Nat. Biotechnol.* **2003**, *21*, 399.
(21) D'Souza, A. J. M.; Schowen, R. L.; Topp, E. M. *J. Controlled Release* **2004**, *94*, 91.
(22) Kubin, A.; Meissner, P.; Wierrani, F.; Burner, U.; Bodenteich, A.; Pytel, A.; Schmeller, N. *Photochem. Photobiol.* **2008**, *84*, 1560.
(23) Zheng, Y.; Huang, X.; Wang, Y.; Xu, H.; Chen, X. *J. Appl. Polym. Sci.* **2009**, *113*, 736.
(24) Mishra, A.; Ram, S.; Ghosh, G. *J. Phys. Chem. C* **2009**, *113*, 6976.
(25) Mishra, A.; Ram, S.; Fecht, H.-J. *J. Nanosci. Nanotechnol.* **2009**, *9*, 4342.
(26) Mishra, A.; Ram, S. *J. Chem. Phys.* **2007**, *126*, 084902.
(27) Mishra, A.; Srivastava, V. K.; Ram, S. *J. Mol. Liq.* **2008**, *137*, 58.
(28) Fujihara, S.; Kitta, S. *Chem. Phys. Lett.* **2004**, *397*, 479.
(29) Carotenuto, G.; Nicolais, L. *Compos., Part B: Eng.* **2004**, *35*, 385.
(30) Skrabalak, S. E.; Au, L.; Li, X.; Xia, Y. *Nat. Protocols* **2007**, *2*, 2182.
(31) Liu, L.; Wei, T.; Guan, X.; Zi, X.; He, H.; Dai, H. *J. Phys. Chem. C* **2009**, *113*, 8595.
(32) Manzoor, K.; Vadera, S. R.; Kumar, N.; Kutty, T. R. N. *Solid State Commun.* **2004**, *129*, 469.
(33) Taylor, L. S.; Langkilde, F. W.; Zografi, G. *J. Pharm. Sci.* **2001**, *90*, 888.
(34) Yamashita, K.; Kuro, T.; Oe, K.; Yanagi, H. *Appl. Phys. Lett.* **2006**, *88*, 241110.
(35) Chin, W. W. L.; Thong, P. S. P.; Bhuvaneswari, R.; Soo, K. C.; Heng, P. W. S.; Olivo, M. *BMC Med. Imag.* **2009**, *9*, 1.
(36) Chen, E.; Ju, J.; Yang, C.; Horng, S.; Tseng, S.; Meng, H.; Shu, C. *Appl. Phys. Lett.* **2008**, *93*, 063304.
(37) Colthup, N. B. Daly, L. H., Wiberley, S. E. *Introduction to Infrared and Raman Spectroscopy*; Academic Press: New York, 1975.

JP906765X